Optimal comfortability control of hybrid electric powertrains in acceleration mode

Bo ZHANG[1*], Yahui ZHANG[1], Jiangyan ZHANG[2] & Tielong SHEN[1]

[1]*Department of Engineering and Applied Sciences, Sophia University, Tokyo* 102-8554, *Japan;*
[2]*College of Mechanical and Electronic Engineering, Dalian Minzu University, Dalian* 116600, *China*

Abstract This paper presents a control design approach for optimizing the comfortability of hybrid electric powertrains in acceleration mode. A parallel hybrid electric vehicle powertrain system with two motors and a single turbo-charged engine is considered. In acceleration mode, it is assumed that the desired acceleration rate cannot be satisfied by using the electrical motor individually. The first challenge is managing the combustion engine to assist power generation and power split such that the system satisfies comfortability, and the second challenge is modeling the comfortability (e.g., analytically describing the human feeling). This paper exploits a black-box module typically used in the automotive industry to quantitatively evaluate comfortability. A genetic algorithm is applied to find the optimum power split and gear schedule that can improve the comfortability evaluated by the module in acceleration mode. The simulation results conducted on a simulator with a practical background demonstrate the significance of the proposed design approach.

Keywords ride comfortability, black-box module, hybrid electric vehicles (HEVs), genetic algorithm (GA), acceleration mode

1 Introduction

Automobiles have become a necessity with imperceptible influence, promoting the development of transportation at the expense of consuming plenty of fossil fuel and contributing to air pollution [1, 2]. A hybrid electric vehicle (HEV) is a type of new energy automobile that has attracted significant attention in recent decades because of its potential ability to reduce fuel consumption. HEVs are usually classified into three categories according to their architectures [3]: (1) parallel HEV; (2) series HEV; and (3) power-split HEV. The fundamental configuration of a typical hybrid powertrain system includes a traditional internal combustion engine, clutch, battery, and an electric machine. The electric machine serves as an extra energy source because of its ability to recover energy; hence, it can either assist the engine or work separately. Therefore, most studies on HEVs have focused on the energy management strategy (EMS) for optimizing power split between energy sources to satisfy a driver's demand.

A wide variety of optimization algorithms for HEV control have been published. Among them, dynamic programming (DP) is often used as a benchmark by providing a globally optimal solution offline. Several studies have used DP for more extensive applications on HEVs [4, 5]. However, DP cannot be applied in practice because a predefined driving route is required. As such, optimization-based controllers that can be implemented online have attracted attention in recent years. Equivalent consumption minimization strategy (ECMS) is an instantaneous optimization that determines an equivalent factor that converts the battery energy to fuel such that the fuel consumption is minimized. Some papers have focused on finding adaptive laws to tune the equivalent factor online [6, 7]. Musardo et al. [8] demonstrated that ECMS can perform very close to the global optimum obtained by DP. Model predictive control (MPC) is another promising approach that is popularly used in EMS by solving a nonlinear optimization problem

---

* Corresponding author (email: zhangbo@eagle.sophia.ac.jp)

over a finite horizon. In [9], a hierarchical control strategy that considers battery aging was proposed to improve fuel economy with the controller designed under the MPC scheme. Because of its characteristics of predicting the future system behavior, MPC is usually combined with other prediction schemes, such as neural network-based velocity prediction, model-based traffic flow prediction, and extreme learning machine-based torque demand prediction [10–12]. Moreover, other research efforts for EMS, such as reinforcement learning, fuzzy control, and logical model-based approaches, have also been proposed in the last few years [13–15].

It should be noted that the above mentioned studies focused on optimization strategy and fuel efficiency without considering human sensory evaluation. However, some studies have indicated that uncomfortable driving may cause traffic accidents and may lead to negative effects on the driver or passengers [16]. For a traditional automobile with a single energy source, vehicle ride comfort is usually evaluated in terms of stability performance [17, 18]. Discontinuous dynamics during mode transitions of the different architectures of a hybrid powertrain system usually results in severe jerk and unpleasant ride feeling. Wang et al. [19] proposed a dual-loop self-learning fuzzy control framework to manage the gear-shift process. The designed controller moves the gear position as fast and smoothly as possible, improving ride comfort to some extent. In addition, it has been suggested that both jerk and acceleration contribute significantly to the performance of ride comfort [20]. In general, an electric motor cannot provide enough power during acceleration. The management of the combustion engine, such as the intervention time and the power distribution, contributes to the rate of acceleration and leads to a different driving feeling. Some existing studies about the ride comfort of HEVs with different mode schedules have only considered vehicle acceleration as a measure of riding sensation. For instance, Luo et al. [21] introduced vehicle acceleration into the control constraints to keep it in a reasonable interval. They found that ride comfort was indirectly improved by generating a flat acceleration series. Tajeddin et al. [22] optimized the energy, safety, and comfort by considering the fuel consumption, velocity tracking, and acceleration restriction in the cost function. However, only a few studies have quantitatively evaluated the comfortability. In addition, the variation in rotational speeds during the mode shift of a hybrid powertrain has also been considered as a crucial factor that affects ride comfort. The reasonable variation could prompt a vehicle to avoid an unpleasant ride comfort and vehicle jerk [23].

In summary, energy management is inevitable during the acceleration process because of the characteristics of the HEV powertrain system. The noticeable jerk or torque fluctuation caused by the operations lead to an uncomfortable driving sensation. Therefore, a reasonable arrangement of the power generated by multiple energy sources is needed that can improve system comfortability. However, the main challenge is modeling and evaluating ride comfort directly. This work aims to address these issues to improve ride comfort and hold a smooth transition operation during the desired acceleration process. The main contributions of this work are as follows. A parallel HEV powertrain model with two motors and a single turbo-charged engine is built. Then, a module for comfort evaluation is presented to quantitatively describe the performance of ride comfort; it is a black-box module designed by experts from the Toyota Research and Development Center. Because the evaluation function is an implicit function with respect to acceleration and jerk, a genetic algorithm (GA) technique is employed to find the optimal power split and gear schedule that satisfy the desired constraints in acceleration mode. As a result, this paper provides a novel optimal ride comfortability control scheme for a hybrid powertrain system with two motors. Moreover, the black-box module of the evaluation function can reflect human senses quantitatively.

The rest of the paper is organized as follows. Section 2 discusses the built parallel HEV powertrain model and the optimization problem. Section 3 introduces the GA for solving the formulated optimization problem. Section 4 describes the simulations and provides a discussion of results. Finally, Section 5 concludes this work.

2 Hybrid powertrain model and optimization problem

2.1 Powertrain model

A parallel HEV uses both an electric motor and a combustion engine to deliver power to the vehicle wheels; hence, it is suitable for passenger cars. The architecture of the considered parallel HEV powertrain is shown in Figure 1. The system comprises two motors (MG1 and MG2) and a turbo-charged engine, where MG1 and MG2 have different motor characteristics. The combustion engine and MG1 are coaxially
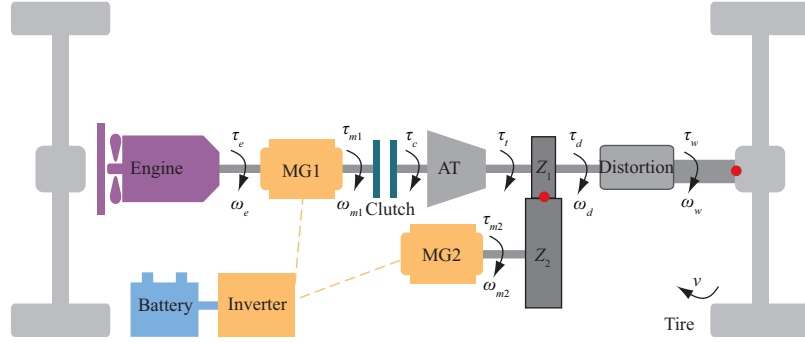
Figure 1 (Color online) Structure of the powertrain system.

connected to the gear box with a clutch. The propulsion torques from the motors and engine are coupled and transmitted to the drive shaft through the differential gear. The variables in Figure 1 have the following meanings: τ_e, τ_{m1}, and τ_{m2} are the torques of the engine, MG1, and MG2, respectively; ω_e, ω_{m1}, and ω_{m2} are the speeds of the engine, MG1, and MG2, respectively; τ_c and τ_t are the input and output torques of the gear box, respectively; τ_d and τ_w are the input and output torques of the differential gear, respectively; ω_d and ω_w are the relevant rotation speeds, respectively; and v is the longitudinal speed of the HEV.

It should be noted that a turbo-charged engine is applied as an energy source. The components of a turbo-charged engine include a turbine and an air compressor, which are used to efficiently harness the exhausted gas emitted from the engine. Because more air enters the cylinders, more power can be generated by the engine. Compared to a conventional naturally-aspirated (NA) engine, a turbo-charged engine provides greater output torque and better fuel economy. The air is drawn into the engine by natural air pressure, while the targeted engine can utilize a turbo to hasten the process. In brief, a turbo-charged engine can significantly increase the engine power and torque at the same emission and can generate power more economically. Moreover, it also addresses environmental protection issues in modern society due to its ability to reduce fuel consumption per unit of power to a greater extent than NA engines. Therefore, turbo-charged engines are popularly used in modern automobiles for reducing emissions and improving fuel economy.

We use CL $= 0$ to denote the clutch is off and CL $= 1$ means the clutch is on. According to Newton's second law and the powertrain structure, the dynamics of the powertrain system shown in Figure 1 is derived as the following equations.

(a) CL $= 0$:

$$
\begin{cases}
\left[I_{\Sigma d_2}\eta_f G_f^2 + (I_{\Sigma\omega} + R_{\text{tire}}^2 M)\right]\dot{v} = \dfrac{\eta_f G_f G_m \tau_{m2}}{R_{\text{tire}}} - F(v), \\
(I_e + I_{m1})\dot{\omega}_e = \begin{cases} 0, & \text{if } \tau_{m1} \leqslant |\tau_e|, \\ \tau_e + \tau_{m1}, & \text{otherwise}, \end{cases} \\
\omega_{m2} = G_m G_f \dfrac{v}{R_{\text{tire}}};
\end{cases}
\tag{1}
$$

(b) CL $= 1$:

$$
\begin{cases}
\left[(I_{\Sigma d_1} + I_{\Sigma d_2})G_f^2\eta_f + (I_{\Sigma\omega} + R_{\text{tire}}^2 M)\right]\dot{v} = \dfrac{\eta_f G_f\left[\eta_t i_g(\tau_e + \tau_{m1}) + G_m \tau_{m2}\right]}{R_{\text{tire}}} - F(v), \\
\omega_{e/m1} = i_g(t)G_f\dfrac{v}{R_{\text{tire}}}, \\
\omega_{m2} = G_m G_f\dfrac{v}{R_{\text{tire}}},
\end{cases}
\tag{2}
$$

where I denotes the rotational inertia of the relevant mechanical structure, $I_{\Sigma d1}$, $I_{\Sigma d2}$, and $I_{\Sigma w}$ denote the accumulated inertia functions of the components, which are presented as $I_{\Sigma d1} = (I_e + I_{m1})\eta_t i_g^2$, $I_{\Sigma d2} = I_d + I_{m2}G_m^2$ and $I_{\Sigma w} = \eta_f G_f^2 I_{z1} + I_{z2}$, respectively, M, R_{tire} and η_f represent the vehicle mass, the radius of the tire and the transmission efficiency, respectively, i_g and η_t denote the gear ratio and efficiency of the gear box, and $F(v)$ is the road load that can be written as

$$
F(v) = \mu_r mg\cos\theta + \frac{1}{2}\rho A C_d v^2 + mg\sin\theta,
\tag{3}
$$

(a)
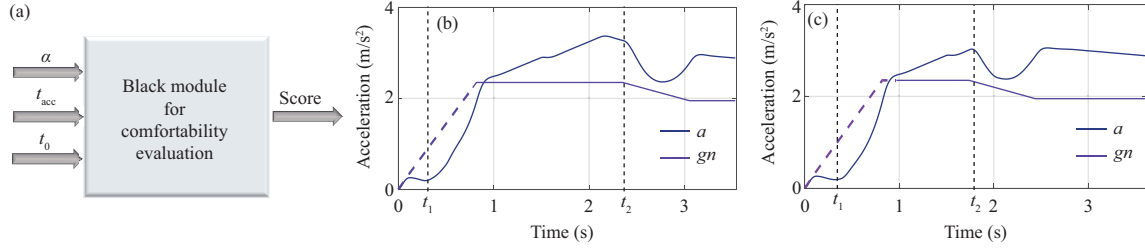
Figure 2 (Color online) The visual examples of human feeling function. (a) The structure and application of the function block; (b) the acceleration curve with score = 60.5141; (c) the acceleration curve with score = 11.7848.

where ρ, A, and C_d denote the air density, the frontal area of the vehicle, and the air drag coefficient, respectively, μ_r and g are coefficients of rolling resistance and gravitational acceleration, and θ is the road slope. It should be noted that the powertrain dynamics (1) and (2) are derived under the assumption that all connections are rigid.

In addition, the power loss is inevitable during charging or discharging in the battery. Define the loss power of MG1 and MG2 as $P_{m1,\text{loss}}$ and $P_{m2,\text{loss}}$, respectively. The power loss is governed by the speed and torque of the motors. For simplified calculation, the power loss of the two motors can be modeled based on experimental data and be expressed as the following polynomial function,

$$P_{m1,\text{loss}} = c_1 \tau_{m1} + c_2 \omega_{m1} + c_3 \tau_{m1} \omega_{m1} + c_4 \omega_{m1}^2, \tag{4}$$

$$P_{m2,\text{loss}} = d_1 \tau_{m2} + d_2 \omega_{m2} + d_3 \tau_{m2} \omega_{m2} + d_4 \omega_{m2}^2 \tag{5}$$

with constant parameters c_i and d_i, $i = \{1, 2, 3, 4\}$.

2.2 Comfortability evaluation

Most studies in the automobile control field have applied the frequency response function and total weighted acceleration root-mean-square value to evaluate driving comfortability. The response function focuses on the effect of the vehicle body structure, such as the stiffness and damping of the suspension system, on ride comfort. It is widely used in conventional internal combustion engine vehicles; however, it cannot analyze ride comfort in HEVs. In addition, ride comfort is observed by analyzing the amplitude-frequency characteristic without intuitive results. Theoretically, it is difficult to describe human feeling and model ride comfort. However, in industries, a black-box module has been built to quantitatively evaluate ride comfort by providing a numerical score with respect to the specific inputs.

To evaluate ride comfort, a human feeling function has been presented by experts and engineers from Toyota; this function considers the acceleration time, acceleration, and jerk. However, it cannot be expressed explicitly. The black-box module for comfortability evaluation is shown in Figure 2(a), where the inputs of the block are the acceleration time vector t_{acc}, the acceleration vector a, and the start time of acceleration t_0; the output is a score in the range $[0, 100]$. The score corresponds to an evaluation index of ride comfort such that a higher score means higher comfortability. It should be noted that the block can only be used to calculate the index with a series of acceleration and time as inputs. To better explain this, different acceleration curves with different scores are shown in Figures 2(b) and (c), where the blue and purple lines denote the acceleration process and gear schedule, respectively. The acceleration processes shown in Figures 2(b) and (c) have identical initial speeds but the index scores are different; i.e., 60.5141 and 11.7848, respectively. These results mean that ride comfort of the acceleration curve in Figure 2(b) is much better than that in Figure 2(c). Moreover, it should be noted that the only differences between Figures 2(b) and (c) are the gear changing time t_2 and the acceleration curve, while the terminal velocity and the whole acceleration horizon are predefined.

2.3 Optimal control problem

In this work, we aim to determine the optimal second shifting time, gear schedule, and power split between the two motors during acceleration to improve the ride comfort. It is assumed that the electric motors are unable to generate enough power for the acceleration. To correspond to the actual driving requirements, the throttle of the engine is required to be fully open after ignition. For improving the engine efficiency during the acceleration process, gear shifting is necessary after the engine starts. Therefore, the combined
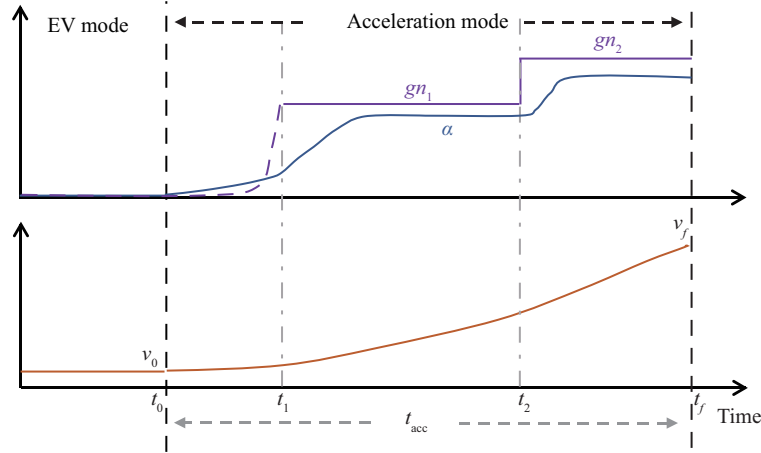
Figure 3 (Color online) The comfortability problem in acceleration mode.

management including the power split, the gear schedule, and the engine assist is crucial for the better driving feeling.

The proposed acceleration process is shown in Figure 3, where the blue line a represents the acceleration, the purple line gn represents the gear schedule, and the orange line represents the velocity curve. The powertrain system operates at a constant speed v_0 under the electric vehicle (EV) mode; i.e, MG2 provides the power. The acceleration process from t_0 to t_f can be described as follows. At the initial time t_0, the vehicle begins to speed up to a specified terminal velocity v_f under the HEV mode. Here, t_1 and t_2 denote the first and second shifting time. During the acceleration process, the motors and engine work together to propel the vehicle. Although the engine is on from the initial time t_0, it is allowed to provide power until the engine speed reaches a reasonable value at time t_1. An initial gear number gn_1 is chosen at time t_1 with the clutch being on at this point. Then, at time point t_2, another gear number gn_2 is chosen to obtain a comfortable acceleration. The vehicle speeds up to the terminal velocity v_f at the terminal time t_f; note that t_f is a specified value. Moreover, the whole acceleration time is denoted as t_{acc} and the initial gear schedule gn_1 is given to reduce mechanical friction in acceleration mode. Thus, the power split ρ between the two motors, the second shifting time t_2, and the gear schedule gn_2 influencing the acceleration curve should be optimized during the acceleration process.

GA is a nature-inspired search-based algorithm used in solving combinatorial optimization problems. The parameters in the considered optimization problem should be able to maximize/minimize the output of the black box [24, 25]. Here, the method is applied to optimize an unknown cost function. A GA-type control scheme is proposed to maximize the index of the comfortability evaluation function. The system block diagram of the GA-based optimal comfortability system is illustrated in Figure 4, where the left block with a blue undertone represents the basic optimization process of the GA approach and the right block with a gray undertone represents the evaluation process. The block is designed for calculating the objective function and evaluating the fitness value with the proposed parallel HEV model and implicit comfortability evaluation function. The initial population of the algorithm is randomly generated based on several parameters within a predefined range. The initial population includes a given number of individuals. For each individual, the objective function value is calculated and a fitness value with respect to each individual is obtained to validate its performance. The calculation process of the objective function is shown in the right part of the flowchart. The outputs of each individual are the control inputs, which include the power split ρ, the second shifting time t_2, and the gear schedule gn_2. Then, the acceleration curve and time can be provided. The related sequences describing the acceleration process are fed into the proposed black-box module to generate an index score for comfortability evaluation. The score is used to evaluate the fitness of each individual. After completing the block of fitness evaluation, basic GA operations are performed. Then, a new population is formulated to execute the new iteration process. Detailed physical meanings of the parameters in Figure 4 are given in the following section.

Moreover, the powertrain dynamics should satisfy the physical constraints. The electric motors should
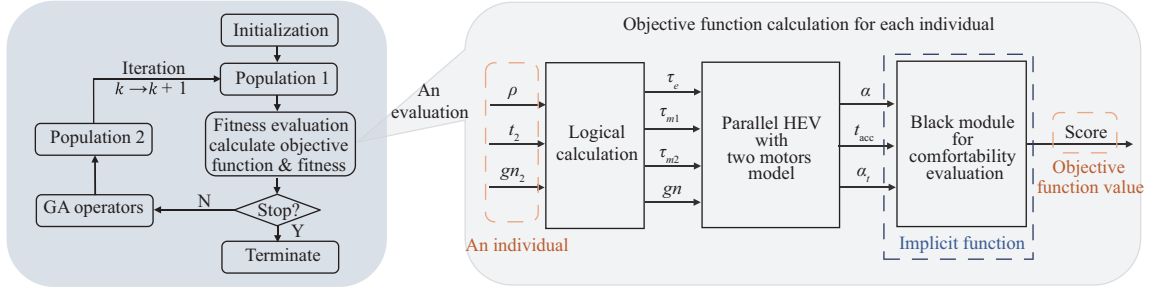
Figure 4 (Color online) Block diagram of the proposed design approach.

satisfy the corresponding characteristic curves as follows:

$$
\begin{aligned}
\tau_{\mathrm{m1,min}} &\leqslant \tau_{m1} \leqslant \tau_{\mathrm{m1,max}}, \\
\tau_{\mathrm{m2,min}} &\leqslant \tau_{m2} \leqslant \tau_{\mathrm{m2,max}}, \\
P_{m1} &+ P_{m1,\mathrm{loss}} + P_{m2} + P_{m2,\mathrm{loss}} = P_{\mathrm{battery}},
\end{aligned}
\tag{6}
$$

where P_{m1} and P_{m2} represent the power of MG1 and MG2, respectively, $P_{m1,\mathrm{loss}}$ and $P_{m2,\mathrm{loss}}$ are the power loss which are modeled as (4) and (5), P_{battery} is the rated power of the battery, it means that the output power of MG1 and MG2 should be satisfied by the battery rated power, and "max/min" represents the maximum/minimum torque of the motors. In addition, the turbo-charged engine has to follow the engine characteristic,

$$
\omega_{e,\mathrm{min}} \leqslant \omega_e(t) \leqslant \omega_{e,\mathrm{max}}.
\tag{7}
$$

Finally, the optimization problem is formulated as follows:

$$
\max_u J(a)
$$

$$
\text{s.t.}
\begin{cases}
[\dot{v}(t), \dot{\omega}_e(t)]^{\mathrm{T}} = f[\tau_e(t), \tau_{m1}(t), \tau_{m2}(t), gn_2, t_2], \\
a(t) = \dot{v}(t), \\
v(t_0) = v_0, \quad v(t_f) = v_f, \\
v_f = v_0 + \Delta v, \quad \Delta v > 0, \\
P_{m1}(t) = \rho(t) P_{\mathrm{battery}}, \\
P_{m2}(t) = \dfrac{P_{\mathrm{battery}} - P_{m1}(t) - P_{m1,\mathrm{loss}}(t)}{\omega_{m2}(t)} - P_{m2,\mathrm{loss}}(t), \\
\tau_{\mathrm{m1,min}}(t) \leqslant \tau_{m1}(t) \leqslant \tau_{\mathrm{m1,max}}(t), \\
\tau_{\mathrm{m2,min}}(t) \leqslant \tau_{m2}(t) \leqslant \tau_{\mathrm{m2,max}}(t), \\
\tau_e(t) = \tau_{e,\mathrm{max}}(t), \\
\omega_{e,\mathrm{min}} \leqslant \omega_e(t) \leqslant \omega_{e,\mathrm{max}}, \\
t_f \leqslant t_{\mathrm{max}}, \\
0 \leqslant \rho(t) \leqslant 1, \\
t_1 + 0.7 \leqslant t_2, \quad t_2 + 0.7 \leqslant t_f,
\end{cases}
\tag{8}
$$

where J denotes the unknown human feeling function, and $J : A \to \mathbb{R}$ is a functional on a function space A, $x = [v, \omega_e]^{\mathrm{T}}$ denotes the state variables, and the input $u = [\rho, t_2, gn_2]^{\mathrm{T}}$ represents the power split ratio between the two motors, the second shifting time, and the second gear number, moreover, the powertrain dynamic should satisfy the physical constrains, f represents the powertrain dynamic equations, the physical meaning of the constraints are shown as (1) and (2). This work aims to find a proper input u that can maximize the unknown human feeling function. However, the power split ratio ρ between two motors during the acceleration process is a function, $\rho : [t_0, t_f] \to \mathbb{R}$, where the terminal time t_f should satisfy the condition: $t_f \leqslant t_{\mathrm{max}}$. Consider that a linear delay within 0.7 s of shifting is inevitable for the proposed parallel powertrain structure. Therefore, the time interval between the two shifting should be over 0.7 s. Moreover, τ_e is predefined to be the maximum torque as the throttle of the engine is fully open in acceleration mode, in other words, $\tau_e = \tau_{e,\mathrm{max}}$.
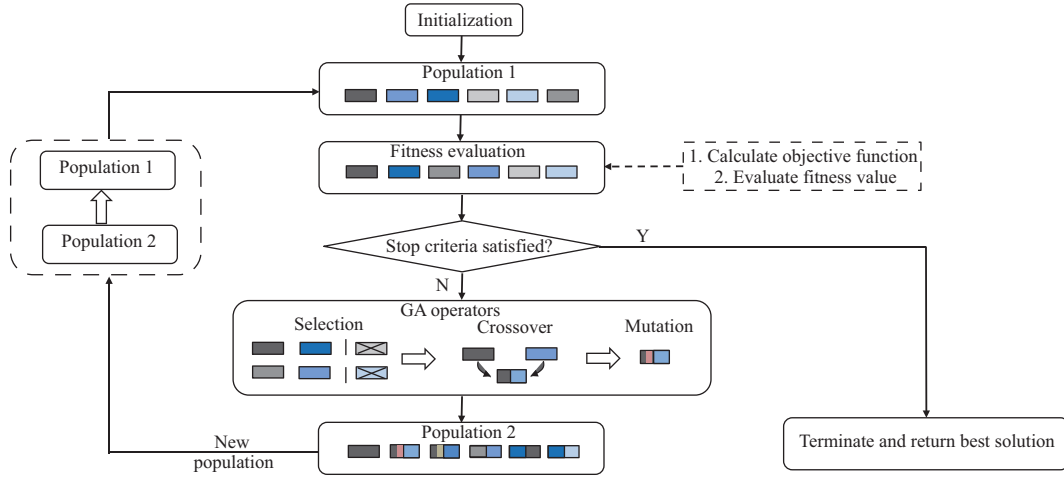
Figure 5 (Color online) The basic structure of the genetic algorithm.

3 GA solution

It should be noted that in this application, the function ρ is discretized in each 0.5 s. Thus the input ρ is discretized into a vector, for instance, ρ is a vector with 12 elements when $t_{\max}$ is set to 6 s. The optimization problem (8) has high dimensions (over ten inputs), and a set of constraints. Moreover, the function is non-analytic and may have multiple local extreme points. Hence, classical optimization methods such as gradient-based methods are incapable to deal with this problem. Heuristic algorithms, for example, genetic algorithm, particle swarm optimization algorithm, and colony optimization algorithm are usually employed to solve such kind of problems. In this application, an enhanced GA is adopted.

GA is a probabilistic global search method that mimics the process of natural biological evolution, i.e., survival of the fittest. The flowchart of GA is shown in Figure 5. The process begins with an initial population of individuals that are randomly generated within the range of parameters. An objective function value of each individual is calculated, and then a fitness value is associated with each individual to evaluate the performance of each individual. Next, three basic genetic operators: reproduction, crossover, and mutation, will be executed. After these operators, a new population is produced, namely, the next generation. The better the fitness value is, the higher the survival probability will be generated. Then, the probability goes into the next generation. GA is a parallel and global search method that searches multiple solutions, so it is expected to achieve a globally optimal solution or a sub-optimal solution.

The crossover and mutation probabilities are two key parameters that significantly affect the searching process of GA. In the early stage of searching, larger crossover and mutation probabilities are beneficial for the diversity of individual. However, in the later stage of searching, large crossover and mutation probabilities may destroy the optimal individual [26]. Moreover, when the best individual or solution is repeated for a number of generations, the algorithm may get stuck at a local minimum. Therefore, adaptive crossover and mutation probabilities are required. Simple but effective adaptive mechanisms are

$$
\begin{aligned}
p_c\left(k\right) &= \left[p_{c0} + \alpha_c k_{\mathrm{frozen}}\right] \times \sqrt{1 - \left(k/k_{\max}\right)^2}, \\
p_m\left(k\right) &= \left[p_{m0} + \alpha_m k_{\mathrm{frozen}}\right] \times \sqrt{1 - \left(k/k_{\max}\right)^2},
\end{aligned}
\tag{9}
$$

where k, k_{frozen}, and $k_{\max}$ are the current generation number, the repeated generation number of the best individual, and the maximum number of generation, respectively, p_{c0} and p_{m0} represent the initial values, and α_c and α_m are tiny constants. One can observe that with increasing generation numbers, the crossover and mutation probabilities tend to decrease. Moreover, the probabilities increase with the increase of repeated generation number of the best individual.

4 Results and discussion

In this work, three types of acceleration process are designed for a velocity increment of $\Delta v = 30$ km/h. First, the simulations for a specific condition are demonstrated with detailed discussion for analyzing

Table 1   List of GA parameters

Parameter	Value
Dimension of input	14
Maximum generation number, $k_{\max}$	100
Population size	70
Initial crossover probability, p_{c0}	0.7
Initial mutation probability, p_{m0}	0.1
Constant, α_c	0.02
Constant, α_m	0.005

Table 2   List of vehicle parameters

| Parameter	Nomenclature	Value	Unit
Vehicle mass	M	2850	kg
Engine inertia	I_e	0.22	kg·m^2
MG1 inertia	I_{m1}	0.06	kg·m^2
Accumulated inertia	$I_{\Sigma d2}$	0.92	kg·m^2
Accumulated inertia	$I_{\Sigma w}$	6.1	kg·m^2
Mechanical parameter	G_m	5.75	–
Mechanical parameter	G_f	3.307	–
Transmission efficiency	η_f	0.87	–
Tire radius	R_{tire}	0.39	m
Air density	ρ	1.2	kg/m^3
Frontal vehicle area	A	2.239	m^2
Drag coefficient	C_d	0.32	–
Rolling resistance	μ_r	0.022	–
Gravity acceleration	g	9.8	N/kg
Gear ratios	i_g	4.93; 3.26; 2.35; 1.95; 1.50;	
		1.20; 1.00; 0.80; 0.66; 0.61	–

Table 3   Optimization process with $v_0 = 70$ km/h

Index value	Shifting time t_2	Gear number gn_2	Terminal time t_f	Iteration step k
75.4020	2.06	4	3.60	1
75.6269	2.03	5	3.88	4
76.2351	2.34	4	3.61	30
76.6778	2.29	4	3.57	40
76.8027	2.33	4	3.57	53
76.8045	2.34	4	3.61	101

the performance of ride comfort and powertrain control. In the first case, the initial velocity is set as $v_0 = 70$ km/h, and the maximum terminal time and desired terminal velocity are set as $t_f = 6$ s and $v_f = 100$ km/h. Based on a number of simulation tests, it is logical to connect the clutch when the engine speed reaches 2000 rpm after ignition, because the speed deviation on both sides of the clutch is in a reasonable interval and the unnecessary friction is avoided at this moment. Therefore, the first shifting time t_1 is defined as the time when the clutch is on. An initial gear $gn_1 = 3$ is given, in other words, the initial gear shift is "3" at the moment t_1. During the acceleration process, another shifting is required, and the vehicle should reach the desired terminal velocity before the time t_f, and the second gear shift gn_2 is generated at the time t_2 by the designed controller. The basic parameters of GA and the main physics parameters of the powertrain system are presented in Tables 1 and 2.

The optimization process using GA is shown in Figure 6. The detailed iteration results for the seeking process of the proposed GA are summarized in Table 3 for analyzing the optimization performance. This condition is marked as Case 1. It can be found from Figure 6 that the index value is much greater as the iteration increases. It means that the ride comfort is improved as the iteration process proceeds step by step. The result shows that after 40 iterations, the increment speed of the index becomes slow. The iteration result trends to the final optimal result $J = 76.8045$.

Moreover, the optimal result of the powertrain control for the index value $J = 76.8045$ can be observed
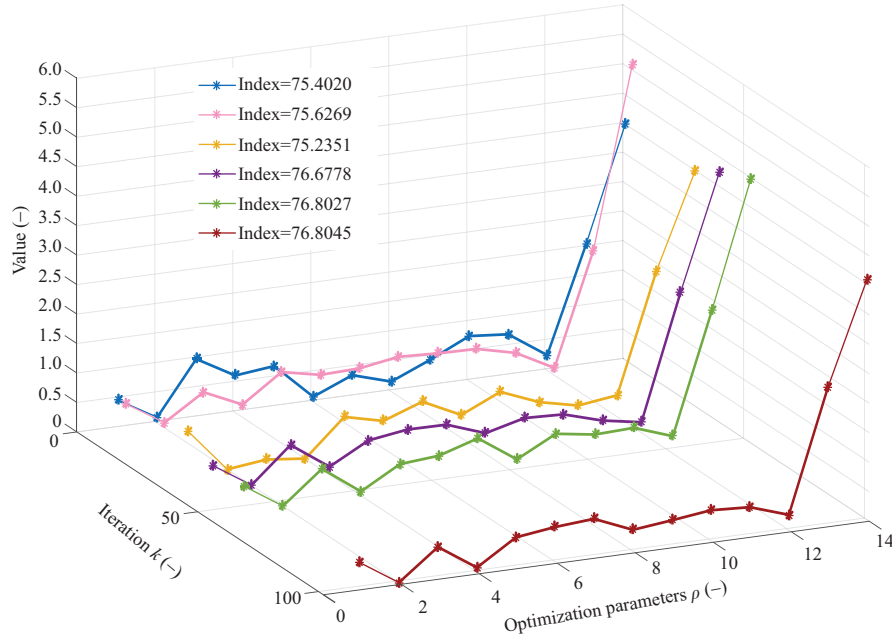
Figure 6 (Color online) The optimization process using GA for $v_0 = 70$ km/h.

from Figures 7 and 8, where the terminal acceleration time is $t_f = 3.61$ s, the second shifting time is $t_2 = 2.34$ s and the second gear number is $gn_2 = 4$. Figure 7 demonstrates the velocity curve, the acceleration changing, and the power split among the energy sources. From Figure 7(d), it can be noted that MG1 operates with the maximum power to drive the engine at the initial stage. It is reasonable to obtain such a result, as the engine and MG1 work under a coaxial structure. Figure 7(c) shows that the engine starts to offset the mechanical resistance at the very beginning. After arriving a certain speed, the engine works under the turbo-charged status to generate the maximal power. It can be observed that the throttle of the engine is fully open in the acceleration mode. During this initial stage, the clutch is off although the engine works. Simulation shows that it consumes 0.33 s when the engine speed reaches 2000 rpm, and the clutch is on at the same time. Figure 7(b) illustrates that the acceleration is quite small before the time t_1, due to that the motors are unable to provide enough power to speed up at such a high driving speed. Therefore, it is inevitable to cooperate the engine and motors for an HEV at such a high initial speed under an acceleration condition. Moreover, it should be noted that the acceleration obviously fluctuates during the second short phase of shifting at 2.34 s. The results are caused by the response of the gear ratio and shifting efficiency, which are shown in Figures 8(a) and (b). Therefore, the fluctuation is inevitable due to the specific physical constraints but could be significantly reduced by a reasonable gear schedule in theory. Furthermore, the power split between the motors shown in Figures 7(d) and (e) reveals that the motors assist the engine to force the powertrain in the acceleration process.

It should be noted that a section of slope function occurs once each action of gear shifting is given in Figure 8(a), i.e., at the time t_1 and t_2. It is caused by the dynamics of the considered hybrid powertrain system. Therefore, a linear delay during 0.7 s occurs when shifting. Moreover, a dynamic process for the efficiency of the gear box exists once the shifting action happens. The process is also realized within 0.7 s. The variation of efficiency η_t follows a nonlinear process as shown in Figure 8(b). However, the acceleration fluctuation at the first shifting time $t_1 = 0.33$ s is much flat. That is due to the following two reasons: (1) the efficiency η_t is monotonically increasing from EV mode to HEV mode; (2) the initial gear ratio is reasonable and the variations of the vehicle state variables are within an acceptable interval when switching the dynamic. Figure 8(c) reveals that the output powers of MG1 and MG2 satisfy the physical characteristic of the battery. The battery capacity determines the ability of the output power provided by the two motors during this acceleration process. Figure 8(d) shows MG1 and the engine always rotate at the same speed because of the coaxial structure. Figure 8(e) represents the speed of MG2 in the acceleration process. Since the vehicle keeps speeding up during this horizon and MG2 maintains working all the time, the speed of MG2 maintains increasing invariably. Moreover, since the initial speed v_0 is relatively high, MG2 works under a high speed zone in this condition.
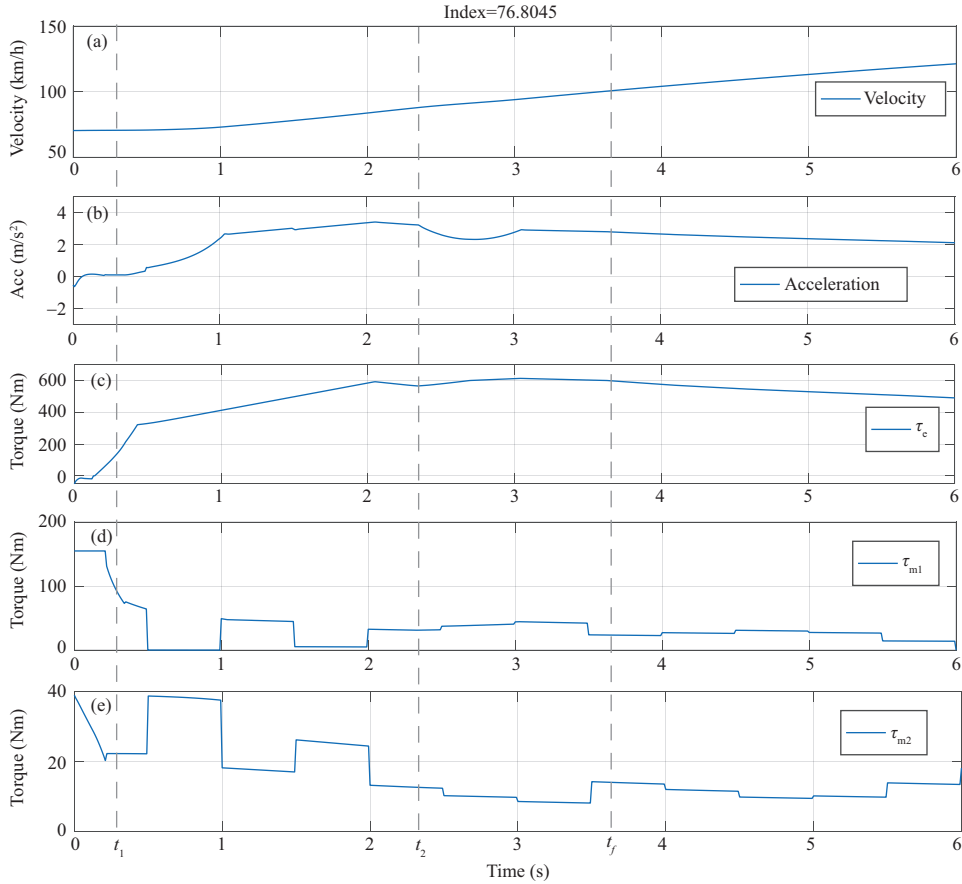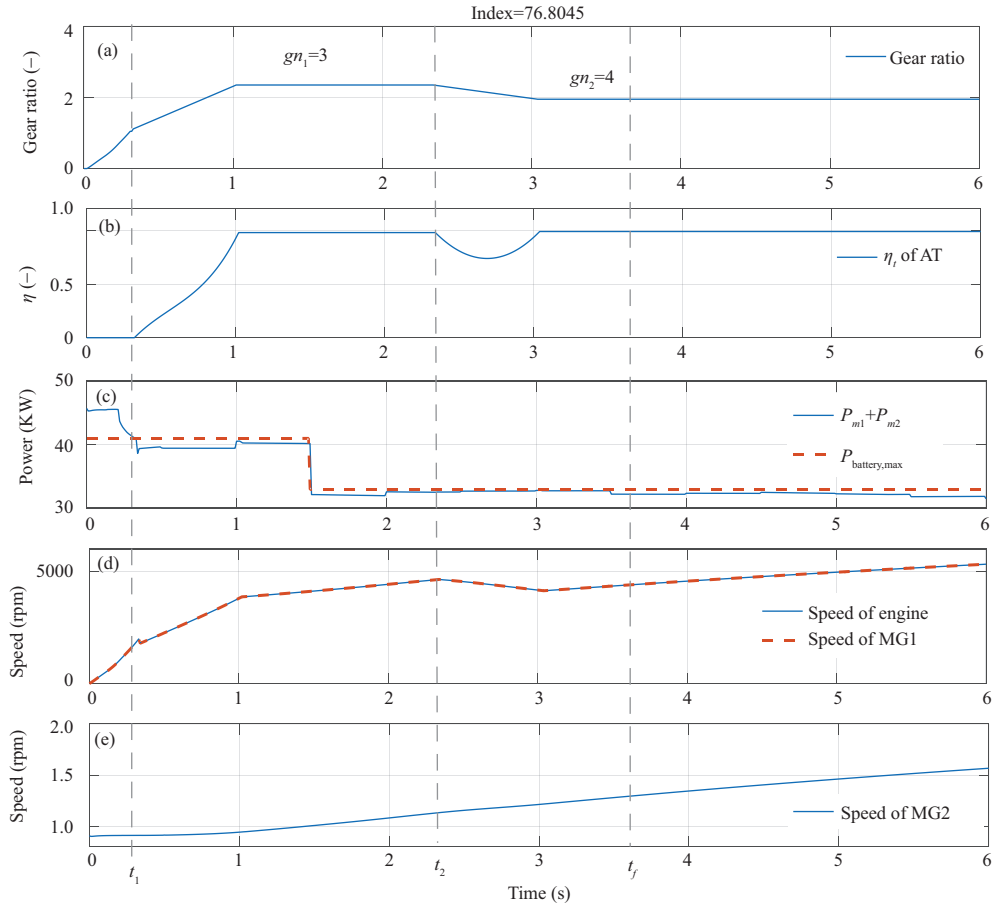
Figure 7 (Color online) The simulation results of a hybrid powertrain. From top to bottom, the figures show the curves including (a) the velocity, (b) the acceleration, (c) the engine torque, (d) the Motor 1 torque, and (e) the Motor 2 torque, respectively.

For a further demonstration of the ride comfort performance of the proposed optimal controller, additional statistical results are shown in the following. To validate the performance of the proposed GA-based strategy on different conditions, more acceleration scenarios are designed. Table 4 shows the optimal results with respect to different initial velocities: $v_0 = 80$ km/h and $v_0 = 90$ km/h. The terminal velocity is set as $v_f = 110$ km/h and $v_f = 120$ km/h, respectively. In Table 4, the terminal time t_f and the second shifting schedule gn_2 are shown. The initial gear gn_1 is given according to the physical condition. It should be noted that the first shifting time t_1 is also defined as the moment that the clutch is on. The initial gear number is given as $gn_1 = 4$ for the two conditions. It can be found from Table 4 that the terminal time t_f for the two cases is much longer than that in the first case with $v_0 = 70$ km/h. The second shifting time t_2 is much closer to the first shifting time t_1. In Case 2, a higher gear shift gn_2 is generated than that in Case 3. It is because that the gear ratio decreases as the gear shift increases, and it is unable to select a high gear shift to reach the desired terminal speed within such a short horizon 6 s. Moreover, the results demonstrate that the feeling index shows potential for reduction as the initial vehicle speed increases.

The simulations for the three acceleration scenarios reveal that a reasonable time of second shifting shows great potential for improving ride comfort. MG2 could provide limited power under the constraints of motor characteristics since the speed of MG2 continuously increases in acceleration mode. The engine provides primary power for speeding up in the above scenarios. In summary, an appropriate gear schedule contributes a lot of effort to a pleasurable ride feeling. The proposed optimal strategy can provide a reasonable power split between the motors and the gear schedules with respect to different acceleration scenarios. Thus, it is concluded that the proposed GA-based optimal comfortability control for HEVs is effective under different acceleration scenarios.

Moreover, some comments should be addressed. First, the clutch dynamic of the powertrain is not considered in this work. It is assumed that the powertrain system is with rigid coupling. Second, this work focuses on investigating the ride comfort during a short-term acceleration process. The problem

Figure 8 (Color online) The simulation results of a hybrid powertrain. From top to bottom, the figures show the curves including (a) the gear ratio, (b) the efficiency of gear box, (c) the power of MG1 and MG2, (d) the speed of MG1 and engine, and (e) the speed of MG2, respectively.

Table 4 Results with different initial speeds

Case	Initial speed v_0 (km/h)	Index value	Shifting time t_2 (s)	Gear gn_1	Gear gn_2	Terminal time t_f (s)
2	80	70.8641	1.26	4	6	5.06
3	90	70.4341	1.43	4	5	5.29

is formulated based on the assumption that the battery can provide enough power during such a short horizon. Therefore, the battery state of charge (SoC) curve during the acceleration is not considered here.

5 Conclusion

In this paper, a GA-based comfortability control scheme for a hybrid powertrain system was presented. The considered HEV transmission system includes two electric motors, a single turbo-charged engine, and a clutch that jointly decides the operating mode (i.e., EV or HEV). Two dynamic models were built to characterize the behavior of the powertrain under different operating modes. The combination of mode shift, power split, and gear schedule resulted in fluctuations in velocity and acceleration, leading to an uncomfortable driving feeling. Thus, an optimal comfortability controller was designed to avoid unreasonable jerk and acceleration and improve ride comfort in acceleration mode. A black-box module was used to quantitatively evaluate ride comfort. Then, a GA technique was used to obtain the optimal power split and gear schedule for an unknown performance function to improve ride comfort. To demonstrate the effectiveness of the proposed strategy, several simulations with different initial conditions were employed under a predefined acceleration scenario. The results show that the proposed strategy can

improve ride comfort and hold smooth transition operations in a specific acceleration mode.

References

1 Gao J W, Li M, Hu Y F, et al. Challenges and developments of automotive fuel cell hybrid power system and control. Sci China Inf Sci, 2019, 62: 051201

2 Chu H Q, Guo L L, Yan Y J, et al. Energy-efficient longitudinal driving strategy for intelligent vehicles on urban roads. Sci China Inf Sci, 2019, 62: 064201

3 Malikopoulos A A. Supervisory power management control algorithms for hybrid electric vehicles: a survey. IEEE Trans Intell Transp Syst, 2014, 15: 1869–1885

4 Zhang J Y, Inuzuka S, Kojima T, et al. Dynamical model of HEV with two planetary gear units and its application to optimization of energy consumption. Sci China Inf Sci, 2019, 62: 222203

5 Vinot E, Trigui R, Cheng Y, et al. Improvement of an EVT-based HEV using dynamic programming. IEEE Trans Veh Technol, 2014, 63: 40–50

6 Sun C, Sun F C, He H W. Investigating adaptive-ECMS with velocity forecast ability for hybrid electric vehicles. Appl Energy, 2017, 185: 1644–1653

7 Han S J, Zhang F Q, Xi J Q. A real-time energy management strategy based on energy prediction for parallel hybrid electric vehicles. IEEE Access, 2018, 6: 70313–70323

8 Musardo C, Rizzoni G, Guezennec Y, et al. A-ECMS: an adaptive algorithm for hybrid electric vehicle energy management. Eur J Control, 2005, 11: 509–524

9 Wu J, Wang X Y, Li L, et al. Hierarchical control strategy with battery aging consideration for hybrid electric vehicle regenerative braking control. Energy, 2018, 145: 301–312

10 Sun C, Hu X S, Moura S J, et al. Velocity predictors for predictive energy management in hybrid electric vehicles. IEEE Trans Control Syst Technol, 2015, 23: 1197–1204

11 Xu F G, Shen T L. Look-ahead prediction-based real-time optimal energy management for connected HEVs. IEEE Trans Veh Technol, 2020, 69: 2537–2551

12 Zhang J Y, Xu F G, Zhang Y H, et al. ELM-based driver torque demand prediction and real-time optimal energy management strategy for HEVs. Neural Comput Applic, 2019, 133: 1–19

13 Liu T, Hu X S, Li S E, et al. Reinforcement learning optimized look-ahead energy management of a parallel hybrid electric vehicle. IEEE/ASME Trans Mechatron, 2017, 22: 1497–1507

14 Zhang J Y, Wu Y H. A stochastic logical model-based approximate solution for energy management problem of HEVs. Sci China Inf Sci, 2018, 61: 070207

15 Wang X Y, Li L, Yang C. Hierarchical control of dry clutch for engine-start process in a parallel hybrid electric vehicle. IEEE Trans Transp Electrific, 2016, 2: 231–243

16 Nandi A K, Chakraborty D, Vaz W. Design of a comfortable optimal driving strategy for electric vehicles using multi-objective optimization. J Power Sources, 2015, 283: 1–18

17 Geweda A E, El-Gohary M A, El-Nabawy A M, et al. Improvement of vehicle ride comfort using genetic algorithm optimization and PI controller. Alexandria Eng J, 2017, 56: 405–414

18 Hegazy S, Sandu C. Vehicle ride comfort and stability performance evaluation. JSAE Tech Paper, 2009, 1: 2859

19 Wang X Y, Li L, He K, et al. Dual-loop self-learning fuzzy control for AMT gear engagement: design and experiment. IEEE Trans Fuzzy Syst, 2018, 26: 1813–1822

20 Grant P R, Haycock B. Effect of jerk and acceleration on the perception of motion strength. J Aircraft, 2008, 45: 1190–1197

21 Luo Y G, Chen T, Zhang S W, et al. Intelligent hybrid electric vehicle ACC with coordinated control of tracking ability, fuel economy, and ride comfort. IEEE Trans Intell Transp Syst, 2015, 16: 2303–2308

22 Tajeddin S, Vajedi M, Azad N L. A Newton/GMRES approach to predictive ecological adaptive cruise control of a plug-in hybrid electric vehicle in car-following scenarios. IFAC-PapersOnLine, 2016, 49: 59–65

23 Zhuang W C, Zhang X W, Yin G D, et al. Mode shift schedule and control strategy design of multimode hybrid powertrain. IEEE Trans Control Syst Technol, 2020, 28: 804–815

24 Pathak I, Vidyarthi D P. A model for virtual network embedding across multiple infrastructure providers using genetic algorithm. Sci China Inf Sci, 2017, 60: 040308

25 Li L, Zhang Y H, Yang C, et al. Hybrid genetic algorithm-based optimization of powertrain and control parameters of plug-in hybrid electric bus. J Franklin Inst, 2015, 352: 776–801

26 Srinivas M, Patnaik L M. Adaptive probabilities of crossover and mutation in genetic algorithms. IEEE Trans Syst Man Cybern, 1994, 24: 656–667